
From Grounding to Skolemization: A Logic-Constrained Vector Symbolic Architecture for Complex Query Answering

Yuyin Lu
Sun Yat-sen University
luyy37@mail2.sysu.edu.cn

Hegang Chen
Sun Yat-sen University
chenhg25@mail2.sysu.edu.cn

Yanghui Rao*
Sun Yat-sen University
raoyangh@mail.sysu.edu.cn

Abstract

Complex Query Answering (CQA) over incomplete Knowledge Graphs (KGs), typically formalized as reasoning with Existential First-Order predicate logic with one free variable (EFO_1), faces a fundamental trade-off between logical soundness and computational efficiency. This work establishes the Grounding-Skolemization dichotomy for systematically analyzing CQA methods through the lens of formal logic. While Grounding-based methods inherently suffer from combinatorial explosion, most Skolemization-based methods neglect to explicitly model Skolem functions and compromise logical consistency. To address these limitations, we propose the Logic-constrained Vector Symbolic Architecture (LVSA), a neuro-symbolic framework that unifies a differentiable Skolemization module and a neural negator, as well as a logical constraint-driven optimization protocol to harmonize geometric and logical requirements. Theoretically, LVSA guarantees universality for all EFO_1 queries. Empirically, it outperforms state-of-the-art Skolemization-based methods and reduces inference costs by orders of magnitude compared to Grounding-based baselines.

1 Introduction

Knowledge Graphs (KGs) are graph-structured databases that represent facts as relationships between entities, which can serve as information retrieval systems for users and downstream task agents [1, 15, 46]. In practical applications, queries issued by users and agents range from simple one-hop lookups to complex queries formalized in Existential First-Order predicate logic with one free variable (EFO_1), involving logical operations of conjunction (\wedge), disjunction (\vee), negation (\neg), and existential quantification (\exists). An example of a complex query is shown in Figure 1.

Prior work conventionally categorizes CQA methods into symbolic, neural, and neuro-symbolic paradigms [45], emphasizing that traditional symbolic approaches [8, 34] based on deterministic search fail to deliver effective solutions for incomplete KGs. In contrast, neural [39, 44, 31] and neuro-symbolic methods [2, 48] achieve superior performance through enhanced generalization capabilities. Motivated by growing demands for trustworthy and interpretable reasoning [43], we introduce a formal logic-grounded taxonomy as a vertical extension of the neural-symbolic taxonomy. By identifying existential variable handling as the critical determinant of CQA efficacy, we

*Corresponding author

partition existing CQA methods into **Grounding-based** and **Skolemization-based** paradigms. This **Grounding-Skolemization dichotomy** elucidates trade-offs between computational efficiency and logical rigor, establishing a unified analytical lens to critique limitations in current CQA methods.

The Grounding-based paradigm operates by grounding EFO_1 formulas into propositional logic through candidate enumeration. Representative Grounding-based methods [2, 48, 5, 42] employ fuzzy logic [26] to compositionally aggregate atomic formula truth values inferred by neural link predictors [36, 49]. While these neuro-symbolic methods demonstrate strong interpretability, their computational complexity grows exponentially with the number of existential variables and candidate entities, rendering them impractical for large-scale KGs.

Conversely, the Skolemization-based paradigm replaces existential variables with Skolem functions, which offers superior reasoning efficiency by relaxing logical equivalence. Given the anticipated growth of KGs' scales [19], the Skolemization-based paradigm represents a critical research frontier. Contemporary methods [17, 31, 47, 4, 39, 44] approximate these Skolem functions through geometric operations in embedding spaces and neural networks. However, after the initial attempt in LogicE [22], subsequent works neglect formal analysis of their logical underpinnings, particularly the failure to enforce inherent constraints of Skolem functions and logical operations. This oversight reduces them to neural approximations lacking guaranteed logical coherence.

This work first conducts a formal analysis of existing CQA methods through the proposed Grounding-Skolemization dichotomy, regarding their tradeoffs between logic rigor and efficiency. Building on these insights, we propose **Logic-constrained Vector Symbolic Architecture (LVSA)**², a novel neuro-symbolic approach that synergizes the logical framework based on Skolemization with the operational principles of Vector Symbolic Architectures [33], achieving the dual advantages of logic rigor and computational efficiency. Specifically, LVSA leverages VSA's highly efficient arithmetic operations over distributed vector representations to model relational projection and basic logical operations, which enables fast inference while maintaining a high degree of transparency. Based on VSA's modular framework, we introduce a differentiable Skolemization module that explicitly enforces logical dependencies and a neural negator integrated with logic-driven regularization terms, to address the challenge of modeling Skolem functions and negation in vector spaces. Theoretically, we prove that our approach guarantees universal applicability to arbitrary EFO_1 queries. Empirically, comprehensive evaluations demonstrate significant improvements over state-of-the-art Skolemization-based methods while achieving up to orders of magnitude acceleration compared to Grounding-based counterparts. Additionally, our LVSA exhibits stronger generalization capabilities for more challenging CQA tasks with insufficient prior knowledge.

2 Preliminary

2.1 Problem Formalization

A **Knowledge Graph (KG)** can be denoted as $\mathcal{G} = \{\mathcal{V}, \mathcal{R}, \mathcal{E}\}$, where \mathcal{V} and \mathcal{R} are the sets of all entities and relations, respectively, and $\mathcal{E} \subseteq \mathcal{V} \times \mathcal{R} \times \mathcal{V}$ is a set of true assertions in the form of triples. Under the open-world assumption [32], an assertion triple of $(h, r, t) \notin \mathcal{E}$ with $h, t \in \mathcal{V}$ and $r \in \mathcal{R}$ may also be true.

Complex Queries on KGs can be formalized as **Existential First-Order predicate formulas with one free variable (EFO₁)**. Formally, a valid EFO_1 query Q consisting of a non-variable (anchor entity) set $\mathcal{V}_a \subseteq \mathcal{V}$, an existential variable set $\mathcal{V}_\exists = \{V_1, V_2, \dots, V_k\}$, and a free variable $V_?$, can be defined in the Disjunctive Normal Form (DNF) as follows:

$$Q[V_?] = V_? : \exists V_1, \dots, V_k : c_1 \vee c_2 \vee \dots \vee c_n, \quad (1)$$

²The source code of our LVSA is available at <https://anonymous.4open.science/r/LVSA-110F>.

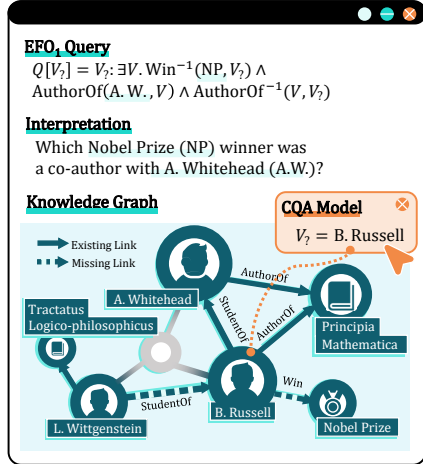


Figure 1: An example of CQA on KGs. -1 denotes the inverse relation.

where each c is a conjunctive query, that is, $c_i = q_{i1} \wedge q_{i2} \wedge \dots \wedge q_{im}$. And each literal q is an atomic formula or its negation, that is, $q_{ij} = r(V', V)$ or $q_{ij} = \neg r(V', V)$, with $V' \in \mathcal{V}_a \cup \mathcal{V}_\exists$, $V \in \{V_\exists\} \cup \mathcal{V}_\exists$, and $r \in \mathcal{R}$. The answer set of the complex query $Q[V_\exists]$ is denoted as $A[Q] \subseteq \mathcal{V}$.

2.2 First-order Predicate Logic Reasoning

A fundamental challenge in first-order predicate logic reasoning lies in handling existentially quantified variables. To address this problem, **Grounding** and **Skolemization** are two primary strategies, respectively based on Herbrand's Theorem and Skolem's Theorem [37].

Definition 1 (Grounding). *Given an EFO₁ formula $\exists V : r(V', V)$, grounding converts it to propositional logic by enumerating all candidate entities for substitutions $\{e/V | e \in \mathcal{V}\}$:*

$$\exists V : r(V', V) \Rightarrow_G \bigvee_{e \in \mathcal{V}} r(V', e). \quad (2)$$

Property 1 (Properties of Grounding). *Let F be an EFO₁ formula and $F \Rightarrow_G F_G$:*

- a. **Equivalence:** F and F_G are equivalent.
- b. **Complexity:** Let F involve k existential variables.
 - (i) *Best-case (Independent variables):* Grounding performs k separate entity substitutions, leading to linear complexity $\mathcal{O}(k|\mathcal{V}|)$.
 - (ii) *Worst-case (Variables with chain of dependency):* Grounding explores all $|\mathcal{V}|^k$ possible paths, leading to exponential complexity $\mathcal{O}(|\mathcal{V}|^k)$.

Definition 2 (Skolemization). *Given EFO₁ formulas $F_D = \exists V_D : r(V', V_D)$ and $F_I = \exists V_I : r(V_I, V')$ with dependent variable V_D and independent variable V_I , Skolemization eliminates the existential quantifier by introducing a Skolem function $f_r(V')$ and a Skolem constant $f_r()$ respectively:*

$$F_D \Rightarrow_S r(V', f_r(V')), F_I \Rightarrow_S r(f_r(), V'). \quad (3)$$

Property 2 (Properties of Skolemization). *Let F be an EFO₁ formula and $F \Rightarrow_S F_S$:*

- a. **Satisfiability:** F is satisfiable $\Leftrightarrow F_S$ is satisfiable. $F_S \models F$ but the converse is not true in general.
- b. **Complexity:** When F involves k existential variables, the complexity of Skolemization is $\mathcal{O}(k)$.

Example 1 Consider the complex query $Q[V_\exists] = V_\exists : \exists V.r_A(A.W., V) \wedge r_A^{-1}(V, V_\exists) \wedge r_W^{-1}(NP, V_\exists)$ illustrated in Figure 1, where r_A and r_W denote the relations of AuthorOf and Win, respectively. Grounding-based reasoning is defined by

$$Q[V_\exists] \Rightarrow_G Q_G[V_\exists] = V_\exists : (r_A(A.W., PM/V) \wedge r_A^{-1}(PM/V, V_\exists) \wedge r_W^{-1}(NP, V_\exists)) \vee (r_A(A.W., B.R./V) \wedge r_A^{-1}(B.R./V, V_\exists) \wedge r_W^{-1}(NP, V_\exists)) \vee \dots \quad (4)$$

In contrast, Skolemization-based reasoning is defined by

$$Q[V_\exists] \Rightarrow_S Q_S[V_\exists] = V_\exists : r_A(A.W., f_{r_A}(A.W.)) \wedge r_A^{-1}(f_{r_A}(A.W.), V_\exists) \wedge r_W^{-1}(NP, V_\exists). \quad (5)$$

3 Limitations of Previous Methods

Grounding-based Methods [2, 48, 5, 42, 23] ground EFO₁ queries into propositional logic formulas and reduce the truth value of each formula into an aggregation of its constituent literals. At the implementation level, the core modules of most Grounding-based methods comprise a neural link predictor $\phi : \mathcal{V} \times \mathcal{R} \times \mathcal{V} \mapsto [0, 1]$ for estimating truth values of literals and fuzzy logic operators $\{\top : \wedge, \perp : \vee, \mathbf{N} : \neg\}$ for truth-value composition, where \perp and \top are specific t-norm/t-conorm pairs [26], and \mathbf{N} is a negator.

Given the equivalence of Grounding (Property 1a) and the truth functionality of propositional logic [13], the grounding-reduction process preserves logical equivalence. However, as shown in Property 1b, most Grounding-based methods [23, 48, 5, 42] (detailed in Appendix A.1) suffer from exponential complexity due to combinatorial explosion, rendering them impractical for queries with

$k > 3$ in various KGs [29]. To alleviate this problem, CQD-Beam [2] employs beam search to prune the size of the search space from $|\mathcal{V}|^k$ to $b^k \cdot |\mathcal{V}|$ with the beam size b . Yet, this greedy strategy trades completeness and accuracy for tractability, which is rigorously quantified in Section 6.4.

Skolemization-based Methods [17, 4, 39, 44, 31, 47] project entities into a particular embedding space and then define logical operations as differentiable geometric transformations within this space. Formally, we denote the embedding function as φ and transformation functions as $\{g_P, g_\wedge, g_\vee, g_\neg, g_\exists\}$, where $g_P, g_\wedge, g_\vee, g_\neg$ are respectively transformation functions for relational projection, conjunction, disjunction, negation, and g_\exists serve as approximations of Skolem functions. By recursively applying these transformations according to a query’s logical structure, these methods derive the query embedding $\varphi(Q)$, thereby facilitating fast querying based on the similarity metric (ϕ_E) defined in the embedding space, where the likelihood of a candidate answer $e \in \mathcal{V}$ is quantified by $E(Q_S[V? = e]) = \phi_E(\varphi(Q), \varphi(e))$.

As formalized in Property 2, Skolemization enhances reasoning efficiency by relaxing logical equivalence to satisfiability, guaranteeing the discovery of at least one valid witness. While this relaxation enables tractable inference, it introduces a local optima risk, limiting the ability of Skolemization-based methods to recover complete answer sets. Concurrently, these methods face the difficulty of simultaneously satisfying logical constraints while maintaining geometric coherence in the embedding space. Specifically, some methods attempt to design sophisticated embedding geometries that inherently encode logical induction biases, e.g., hypercone-structured space of ConE [47] and Beta distribution embedding space of BetaE [31]. However, their reliance on intricate symbolic-geometric operations leads to optimization instability and high computational costs. On the other hand, methods like LMPNN [39] and CLMPT [44] implicitly approximate Skolem functions through message passing over query graphs. While achieving functional approximation, the black-box nature of Graph Neural Networks (GNNs) inherently limits their interpretability [43], as validated in Section 6.6. Due to the theoretical relaxation and practical implementation challenges, current Skolemization-based methods generally underperform Grounding-based approaches in terms of solution quality. However, new CQA benchmarks [16] suggest that previous experimental validation focused on partially observable complex queries that could be answered via 1-hop lookup. Our research further reveals that Skolemization-based methods have stronger generalization capabilities compared to Grounding-based methods in fully unobservable complex queries, demonstrating their value in more challenging real-world applications.

Example 1 (cont.) Considering $V? = \text{B.R.}$, the reasoning algorithm of Grounding-based methods is formalized as follows:

$$E(Q_G[V? = \text{B.R.}]) = (\phi(\text{A.W.}, r_A, \text{PM}) \top \phi(\text{PM}, r_A^{-1}, \text{B.R.}) \top \phi(\text{NP}, r_W^{-1}, \text{B.R.})) \perp \\ (\phi(\text{A.W.}, r_A, \text{B.R.}) \top \phi(\text{B.R.}, r_A^{-1}, \text{B.R.}) \top \phi(\text{NP}, r_W^{-1}, \text{B.R.})) \perp \dots \quad (6)$$

The reasoning algorithm of Skolemization-based methods is defined by

$$\varphi(Q) = g_I(g_P(f_{r_A}(\text{A.W.}) | r_A^{-1}), g_P(\text{NP} | r_W^{-1})), \quad f_{r_A}(\text{A.W.}) \approx g_\exists(\text{A.W.} | Q), \\ E(Q_S[V? = \text{B.R.}]) = \phi_E(\varphi(Q), \varphi(\text{B.R.})). \quad (7)$$

4 Methodology

To enhance reasoning efficiency with logical rigor, we propose the **Logic-constrained Vector Symbolic Architecture (LVSA)**, a novel neuro-symbolic solution to the Skolemization-based CQA paradigm. Unlike prior Skolemization-based methods that rely on intricate geometric embeddings or deep neural architectures, LVSA adopts the Vector Symbolic Architecture (VSA) as its computational foundation, which provides powerful algebraic primitives on simple vector embeddings [33]. The modular design of VSA enables the integration of logic-constrained neural components, including a neural negator and a differentiable Skolemization module. Unlike GNN-based methods that diffusely aggregate neighborhood information without an explicit reasoning order, LVSA’s sequential reasoning process follows the topological ordering of the FOL query’s computation graph. This sequential reasoning, with explicit modeling of Skolem functions, enables causal traceability and enhances interpretability. Further analysis of prior CQA methods and our LVSA can be found in Appendix A.

The key modules of our LVSA can also be summarized as $(\varphi, \{g_P, g_\wedge, g_\vee, g_\neg, g_\exists\}, \phi_E)$. Firstly, we introduce the basic vector symbolic encoding (Section 4.1), followed by a neural negator and

a differentiable Skolemization module (Section 4.2). Then, we present a logic-driven optimization protocol for preserving logical constraints (Section 4.3).

4.1 Basic Vector Symbolic Encoding

Embedding Function (φ): Building on the success of complex-valued vectors in both Knowledge Graph Embedding (KGE) models [36, 24, 34] and VSA [27, 28], we map entities into a complex vector space³. For an entity $e \in \mathcal{V}$, its complex-valued embedding is defined by

$$\varphi(e) = \text{Re}(e) + \text{Im}(e)i, \quad (8)$$

where the trainable real component $\text{Re}(e) \in \mathbb{C}^d$ and imaginary component $\text{Im}(e) \in \mathbb{C}^d$ replace traditional VSA’s random vectors to capture semantic correlation among entities.

Relational Projection (g_P): Through projecting relations into the same embedding space as entities, we can define relational projection by the **Binding** (\otimes) operator, which is implemented as Hadamard product (\odot) between embeddings of the relation ($r \in \mathcal{R}$) and the head entity ($h \in \mathcal{V}$):

$$\begin{aligned} \varphi(r \otimes h) &= \text{Re}(r \otimes h) + \text{Im}(r \otimes h)i \\ &= [\text{Re}(r) \odot \text{Re}(h) - \text{Im}(r) \odot \text{Im}(h)] + [\text{Re}(r) \odot \text{Im}(h) + \text{Im}(r) \odot \text{Re}(h)]i. \end{aligned} \quad (9)$$

Intuitively, binding emphasizes specific attributes of each entity under different relations, e.g., StudentOf \otimes A.W. \approx B.R. and AuthorOf \otimes A.W. \approx PM distinguish A. Whitehead’s roles as an advisor versus an author.

Logical Conjunction (g_\wedge): Inspired by VSA, we model the conjunction operator through **Bundling** ($+$), which is implemented as normalized addition (NormAdd)⁴. Formally, the embedding of a conjunctive query $Q_\wedge = r_1(V'_1, V) \wedge \dots \wedge r_N(V'_N, V)$ is computed as

$$\varphi(Q_\wedge) = \varphi(r_1 \otimes V'_1 + \dots + r_N \otimes V'_N) = \text{NormAdd}[\varphi(r_1 \otimes V'_1), \dots, \varphi(r_N \otimes V'_N)], \quad (10)$$

where the normalization enforces magnitude consistency between inputs and the output. Notably, bundling inherently preserves geometric proximity between output embeddings (superposition) and input embeddings when it satisfies the commutativity and associativity axioms of logical conjunction.

Logical Disjunction (g_\vee): DNF can decompose the answer set of a disjunctive query into a union of the answer sets of its conjunctive sub-queries, i.e., $A[Q] = A[c_1] \cup \dots \cup A[c_n]$ for $Q[V_i]$.

Similarity Measure (ϕ_E): We adopt the real part of the Hermitian inner product as the similarity between complex-valued vectors. Formally, the predicted score of a candidate entity $e \in \mathcal{V}$ for the complex query $Q[V_i]$ is defined by

$$E(Q_S[V_i = e]) = \text{Re} \left(\langle \varphi(Q), \overline{\varphi(e)} \rangle \right) = \text{Re}(Q) \cdot \text{Re}(e) + \text{Im}(Q) \cdot \text{Im}(e), \quad (11)$$

where $\overline{\varphi(e)} = \text{Re}(e) - \text{Im}(e)i$ is the conjugate of $\varphi(e)$.

4.2 Neural Negator and Differentiable Skolemization

Logical Negation (g_-): Modeling semantic inversion in the embedding space while satisfying logical axioms of negation presents fundamental challenges. To address this, we propose a neural negator (MLP_N) trained under logic-driven regularization (detailed in Section 4.3). As negation is more practical when taking a conjunction together, we define the general form of complex queries involving logical negation as $Q_- = Q_\wedge \wedge \neg r_{N+1}(V'_{N+1}, V)$, whose embedding is computed by

$$\begin{aligned} \varphi(\neg(r_{N+1} \otimes V'_{N+1})) &= \text{MLP}_N(\varphi(Q_\wedge) \oplus \varphi(r_{N+1} \otimes V'_{N+1})), \\ \varphi(Q_-) &= \varphi((r_1 \otimes V'_1 + \dots + r_N \otimes V'_N) + \neg(r_{N+1} \otimes V'_{N+1})) \\ &= \text{NormAdd}[\varphi(r_1 \otimes V'_1 + \dots + r_N \otimes V'_N), \varphi(\neg(r_{N+1} \otimes V'_{N+1}))], \end{aligned} \quad (12)$$

where $\text{MLP}_N(\cdot)$ is a feedforward neural network and \oplus denotes embedding concatenation.

³We discuss the intrinsic connections between existing KGE models and VSA in Appendix B.

⁴The detailed design of NormAdd can be found in Appendix C.

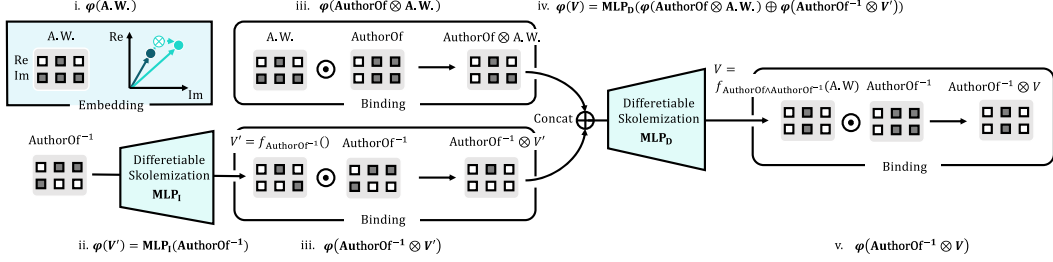


Figure 2: LVSA’s inference process for the subquery of $\exists V.\text{AuthorOf}(A.W., V) \wedge \text{AuthorOf}^{-1}(V, V_2)$.

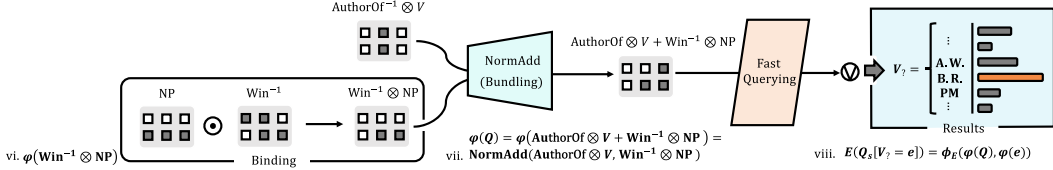


Figure 3: LVSA’s remaining inference process for the sample complex query with the embedding of the subquery $\varphi(\text{AuthorOf}^{-1} \otimes V)$.

Existential Quantification (g_{\exists}): A key contribution of our LVSA lies in explicitly modeling Skolem functions under first-order logical dependencies, which inherently strengthens logic rigor while theoretically guaranteeing universal expressivity for EFO₁ queries.

For independent existential variables V_I , i.e., $\exists V_I : r(V_I, V) \Rightarrow_S r(f_r(), V)$, we generate their embeddings via a relation-aware neural network (MLP_I):

$$\varphi(V_I) = \text{MLP}_I(\varphi(r)). \quad (13)$$

For dependent existential variables V_D , i.e., $F = \exists V_D : r_1(V_1, V_D) \wedge r_2(V_D, V_2) \Rightarrow_S F_S = r_1(V_1, f_{r_1 \wedge r_2}(V_1)) \wedge r_2(f_{r_1 \wedge r_2}(V_1), V_2)$, we first apply the following transformation (\Rightarrow_*) to F :

$$\begin{aligned} F &\Rightarrow_* F^* = \exists V_D, V_I : r_1(V_1, V_D) \wedge r_2^{-1}(V_I, V_D) \\ &\Rightarrow_S F_S^* = r_1(V_1, f_{r_1 \wedge r_2^{-1}}(V_1)) \wedge r_2^{-1}(f_{r_2^{-1}}(), f_{r_1 \wedge r_2^{-1}}(V_1)). \end{aligned} \quad (14)$$

By introducing an auxiliary independent variable V_I , the embedding of V_D can be inferred based on the logical and semantic information from both literals, which is defined as follows:

$$\varphi(V_D) = \text{MLP}_D(\varphi(r_1 \otimes V_1) \oplus \varphi(r_2^{-1} \otimes V_I)). \quad (15)$$

Example 1 (cont.) Figures 2 and 3 illustrate the reasoning workflow of our LVSA for the sample complex query. Panel (i) depicts the geometry in LVSA’s complex vector space. Panels (ii)-(v) illustrate the differentiable Skolemization module’s workflow. Bundling operations are shown in (vi)-(vii), and (viii) demonstrates fast querying based on the similarity metric.

4.3 Logic-Driven Optimization Protocol

The previous sections have detailed the architecture and reasoning workflow of our LVSA. We now introduce the logic-driven optimization protocol for model training. The primary training objective for LVSA is a cross-entropy loss. Given a training batch $\mathcal{B} = \{(Q, t)\}$, the loss enforces higher prediction scores for answer entities $\{t \in A[Q]\}_{(Q,t) \in \mathcal{B}}$ compared to negative samples:

$$\begin{aligned} \mathcal{L}_{\text{CE}}(\mathcal{B}) &= \frac{1}{|\mathcal{B}|} \sum_{(Q,t) \in \mathcal{B}} H(Q, \mathcal{V}) \\ &= \frac{1}{|\mathcal{B}|} \sum_{(Q,t) \in \mathcal{B}} \left[-E(Q_S[V_? = t]) + \ln \sum_{e \in \mathcal{V}} \exp(E(Q_S[V_? = e])) \right]. \end{aligned} \quad (16)$$

To ensure that the neural negator adheres to logical consistency, we impose two key logical properties: **Satisfiability** and **Logical Axioms**. The satisfiability condition requires that for $V = t$ holding $Q_{\neg} \equiv True$, the negator should infer $\neg r_{N+1}(V'_{N+1}, t)$ to be false. In addition, the negator must comply with two fundamental logical axioms: the double negation law ($\neg\neg x \equiv x$) and contradiction law ($\neg x \wedge x \equiv False$). These logical constraints are incorporated into the following loss functions:

$$\mathcal{L}_{NS}(\mathcal{B}_{\neg}; \alpha) = -\frac{\alpha}{|\mathcal{B}_{\neg}|} \sum_{Q_{\neg} \in \mathcal{B}_{\neg}} \ln \sigma [\phi_E(\varphi(\neg(r_{N+1} \otimes V'_{N+1})), \varphi(V))], \quad (17)$$

$$\begin{aligned} \mathcal{L}_{NL}(\mathcal{B}_{\neg}; \beta) = & \frac{\beta}{|\mathcal{B}_{\neg}|} \sum_{Q_{\neg} \in \mathcal{B}_{\neg}} MSELoss(\varphi(\neg\neg(r_{N+1} \otimes V'_{N+1})), \varphi(r_{N+1} \otimes V'_{N+1})) + \\ & MSELoss(\varphi(\neg(r_{N+1} \otimes V'_{N+1})), -\varphi(r_{N+1} \otimes V'_{N+1})), \end{aligned} \quad (18)$$

where $\sigma(\cdot)$ is the sigmoid function and $MSELoss(a, b) = \|a - b\|_2^2$. Besides, α and β are weights of \mathcal{L}_{NS} and \mathcal{L}_{NL} , respectively.

To mitigate overfitting, we adopt a three-stage curriculum learning strategy [6] with gradient back-propagation, structured as follows:

- (i) Train entity and relation embeddings ($\{\varphi(e)|e \in \mathcal{V}\} \cup \{\varphi(r)|r \in \mathcal{R}\}$) using atomic queries (**1p**): $\mathcal{L}_1 = \mathcal{L}_{CE}(\mathcal{B}_{1p})$.
- (ii) Fix pretrained embeddings and fine-tune the differentiable Skolemization module (MLP₁ and MLP_D) on multi-hop queries (**2p** and **3p**): $\mathcal{L}_2 = \mathcal{L}_{CE}(\mathcal{B}_{2p \wedge 3p})$.
- (iii) Optimize the neural negator (MLP_N) on queries involving negation (**2in**), with pretrained parameters frozen: $\mathcal{L}_3 = \mathcal{L}_{CE}(\mathcal{B}_{2in}) + \mathcal{L}_{NS}(\mathcal{B}_{2in}; \alpha) + \mathcal{L}_{NL}(\mathcal{B}_{2in}; \beta)$.

5 Theoretical Analysis

Theorem 1 (Universal Expressivity for EFO₁). *LVSA guarantees universal applicability to all EFO₁ queries over incomplete KGs.*

Proof. We establish universal expressivity through constructive proof. Let $Q[V_?]$ be an arbitrary EFO₁ query, which can be represented as a Directed Acyclic Graph (DAG) $\mathcal{G}_Q = (\mathcal{V}_Q, \mathcal{E}_Q)$ where nodes \mathcal{V}_Q represent (non-)variables and edges \mathcal{E}_Q encode relational projections [42]. Following the topological ordering of \mathcal{G}_Q [14], LVSA computes (non-)variable embeddings sequentially.

Base Case: For anchor entities and independent existential variables, their embeddings are derived by Equations (8) and (13), respectively.

Inductive Step: For each dependent existential variable $V_D \in \mathcal{V}_Q$ with one predecessor u and one successor w , its embedding is computed by Equation (15).

Canonicalization: V_D with multiple dependencies are reduced to this canonical form through algebraic manipulation. Consider V_D with forward (F_D) and backward (B_D) dependencies:

$$F_D = \exists V_D : \bigwedge_{i=1}^N r_{F,i}(u_i, V_D), \quad B_D = \exists V_D : \bigwedge_{j=1}^M r_{B,j}(V_D, w_j). \quad (19)$$

Given $B_D \Rightarrow_* B_D^* = \exists V_D : \bigwedge_{m=1}^M r_{B,m}^{-1}(V_{I,m}, V_D)$, LVSA unifies them via superposition:

$$\begin{aligned} \varphi(F_D) &= \varphi(r_{F,1} \otimes V_{F,1} + \dots + r_{F,N} \otimes V_{F,N}), \\ \varphi(B_D) &= \varphi(r_{B,1}^{-1} \otimes V_{I,1} + \dots + r_{B,M}^{-1} \otimes V_{I,M}), \\ \varphi(V_D) &= \text{MLP}_D(\varphi(F_D) \oplus \varphi(B_D)). \end{aligned} \quad (20)$$

By structural induction on \mathcal{G}_Q 's topology, all EFO₁ constructs are preserved under LVSA's algebraic operations⁵. This preservation enables LVSA to systematically compute embeddings and execute sound logical inference for arbitrary EFO₁ queries. \square

⁵Appendix D provides a case study illustrating this workflow of LVSA.

6 Experiments

6.1 Experimental Settings

Datasets and Evaluation Protocol: We adopt the standard CQA benchmarks established by Ren et al. [31] and the new benchmarks from Gregucci et al. [16], derived from three widely used KGs: FB15k [7], FB15k-237 [35], and NELL995 [40], using their official training/validation/testing splits. Notably, standard benchmarks primarily evaluate performance on partially observable complex queries that could be answered via 1-hop lookup, emphasizing factual recall over reasoning. Conversely, new benchmarks exclusively assess fully unobservable queries requiring compositional reasoning over learned representations. Each benchmark comprises 14 types of complex queries, including 8 types ($2p/3p/ip/pi/up/inp/pin/pni$) with existential variables and 5 types ($2in/3in/inp/pin/pni$) involving logical negation. Detailed statistics and comprehensive query descriptions are provided in Appendix E. Following the evaluation protocol of Ren et al. [31], we compute the filtered Mean Reciprocal Rank (MRR) and Hit at K ($H@K$) by ranking each test query’s non-trivial answers against negative candidates, excluding known true triples from the training/validation sets.

Implementation: LVSA uses two/three-layer feedforward networks with LeakyReLU activations for neural modules. We set the embedding dimension to $d = 1000$ and regularization weights to $\alpha = \beta = 1$. All experiments are conducted on a single Nvidia RTX 3090 GPU integrated with 24GB of memory. More details of experimental settings and hyperparameter sensitivity analysis are in Appendices E and F.

6.2 Main Results

As mentioned in Section 3, direct performance comparisons between Skolemization-based and Grounding-based methods yield limited insights due to their divergent theoretical foundations. Our main experiments therefore focus on evaluating LVSA against Skolemization-based baselines, deferring the analysis of the efficiency-performance tradeoffs with Grounding-based methods to Section 6.4. As shown in Table 1, CQD-CO [2] suffers from an oversimplified approximation of Skolem functions and iterative optimization during inference, leading to limited performance and efficiency. BetaE [31] and ConE [47] struggle to balance geometric properties in their intricate embedding spaces with logical constraints. Meanwhile, LMPNN [39] and CLMPT [44] implicitly model Skolem functions via strong GNNs [41], yet their black-box nature compromises interpretability.

Notably, LVSA demonstrates statistically significant superiority over baselines overall (paired t-test p -value < 0.01 ; see Appendix G for details). Particularly, it excels on conjunction-heavy queries (e.g., $2i$) and negation handling, proving the superiority of binding and bundling implemented by simple algebraic operations, as well as the logically constrained neural negator. However, a minor performance gap persists against GNN-based methods on specific FB15k queries (e.g., $2p$). This is likely due to the inverse relation leakage present in FB15k [35], which allows GNNs to exploit memorization-based shortcuts—a heuristic advantage unavailable to LVSA’s explicit symbolic-geometric reasoning. Additionally, LVSA’s advantages diminish on ip and inp query types when superposition is used as the input to the neural Skolemization module. This suggests that while the current architecture excels at tractable logical compositions, how to enhance its robustness remains an open challenge.

6.3 Results on New Benchmarks

Table 2 shows the results of Grounding-based methods (i.e., GNN-QE [48], QTO [5]) and Skolemization-based methods (i.e., ConE [47], CLMPT [44], LVSA) on the standard and new benchmarks. Δ (%) denotes the performance decline from standard to new setting. Skolemization-based methods experience a significantly smaller performance drop when moving to fully unobservable queries (Avg Δ : 36.5%) compared to Grounding-based methods (Avg Δ : 52.3%). Within the evaluated models, LVSA achieves the highest MRR on unobservable queries while maintaining comparable performance drops to CLMPT, validating its robustness in this challenging CQA setting.

We propose that the performance disparity stems from the fundamental operational differences between the two paradigms. Grounding-based methods achieve completeness by exhaustively searching the KG, allowing them to excel at partially observable queries by perfectly leveraging memorized facts.

Table 1: The MRR (%) results of our LVSA and the existing Skolemization-based baselines. A_p and A_n are the average scores among positive and negative queries, respectively.

Dataset	Model	A_p	A_n	$1p$	$2p$	$3p$	$2i$	$3i$	pi	ip	$2u$	up	$2in$	$3in$	inp	pin	pni
FB15k	CQD-CO	45.3	4.6	89.4	27.6	15.1	63.0	65.5	46.0	35.2	42.9	23.2	0.2	0.2	4.0	0.1	18.4
	BetaE	41.6	11.8	65.1	25.7	24.7	55.8	66.5	43.9	28.1	40.1	25.2	14.3	14.7	11.5	6.5	12.4
	ConE	49.8	14.8	73.3	33.8	29.2	64.4	73.7	50.9	35.7	55.7	31.4	17.9	18.7	12.5	9.8	15.1
	LMPNN	50.6	20.0	85.0	39.3	28.6	68.2	76.5	46.7	43.0	36.7	31.4	29.1	29.4	14.9	10.2	16.4
	CLMPT	55.1	17.9	86.1	43.3	33.9	69.1	78.2	55.1	46.6	46.1	37.3	21.2	22.9	17.0	13.0	15.3
	LVSA	59.9	27.7	89.4	40.6	32.0	80.4	84.2	61.1	43.2	72.0	35.8	41.5	33.7	15.0	17.9	30.4
FB15k-237	CQD-CO	19.8	1.7	46.7	10.3	6.5	23.1	29.8	22.1	16.3	14.2	8.9	0.2	0.2	2.1	0.1	6.1
	BetaE	20.9	5.5	39.0	10.9	10.0	28.8	42.5	22.4	12.6	12.4	9.7	5.1	7.9	7.4	3.5	3.4
	ConE	23.4	5.9	41.8	12.8	11.0	32.6	47.3	25.5	14.0	14.5	10.8	5.4	8.6	7.8	4.0	3.6
	LMPNN	24.1	7.8	45.9	13.1	10.3	34.8	48.9	22.7	17.6	13.5	10.3	8.7	12.9	7.7	4.6	5.2
	CLMPT	25.9	7.9	45.7	13.7	11.3	37.4	52.0	28.2	19.0	14.3	11.1	7.7	13.7	8.0	5.0	5.1
	LVSA	28.8	10.9	49.2	15.8	12.1	41.7	55.1	31.0	19.0	22.5	12.4	12.4	18.3	8.5	7.3	8.0
NELL995	CQD-CO	28.4	1.9	60.8	18.3	13.2	36.5	43.0	30.0	22.5	17.6	13.7	0.1	0.1	4.0	0.0	5.2
	BetaE	24.6	5.9	53.0	13.0	11.4	37.6	47.5	24.1	14.3	12.2	8.5	5.1	7.8	10.0	3.1	3.5
	ConE	27.1	6.4	53.1	16.1	13.9	40.0	50.8	26.3	17.5	15.3	11.3	5.7	8.1	10.8	3.5	3.9
	LMPNN	30.7	8.0	60.6	22.1	17.5	40.1	50.3	28.4	24.9	17.2	15.7	8.5	10.8	12.2	3.9	4.8
	CLMPT	31.3	7.0	58.9	22.1	18.4	41.8	51.9	28.8	24.4	18.6	16.2	6.6	8.1	11.8	3.8	4.5
	LVSA	32.4	9.1	61.0	22.2	18.9	43.6	53.2	31.8	25.0	19.4	16.6	10.1	11.4	11.8	6.1	6.1

In contrast, Skolemization-based methods seek to find at least one valid reasoning path via approximated Skolem functions. This objective inherently requires selective access to relevant memorized facts and compositional reasoning. This fundamental difference makes Skolemization-based methods less reliant on exhaustive memorization and inherently more robust for unobservable queries in real-world scenarios with sparse prior knowledge.

Table 2: Average MRR (%) results across 14 types of complex queries on the standard (A_{part}) and new (A_{full}) benchmarks.

	FB15k-237			NELL995		
	A_{part} (\uparrow)	A_{full} (\uparrow)	Δ (\downarrow)	A_{part} (\uparrow)	A_{full} (\uparrow)	Δ (\downarrow)
GNN-QE	20.9	9.2	55.9	22.1	11.9	46.3
QTO	27.1	9.7	64.3	25.7	14.8	42.6
ConE	17.1	8.5	50.5	19.7	13.8	30.2
CLMPT	19.4	11.3	41.9	22.6	16.7	25.9
LVSA	22.4	12.2	45.6	24.1	18.2	24.6

6.4 Efficiency Analysis

This section evaluates LVSA’s efficiency against the strongest Skolemization-based baseline of CLMPT and the tractable Grounding-based method CQD-Beam [2]. Theoretically, for queries with k existential variables, Skolemization-based methods exhibit $\mathcal{O}(k \cdot cost(g))$ complexity, where $cost(g)$ denotes Skolem function approximation overhead. In contrast, most Grounding-based methods [23, 48, 5, 42] (detailed in Appendix A.1) scale between $\mathcal{O}(k|\mathcal{V}| \cdot cost(\phi))$ and $\mathcal{O}(|\mathcal{V}|^k \cdot cost(\phi))$, with $cost(\phi)$ denoting neural link prediction costs. CQD-Beam leverages beam search to reduce complexity to $\mathcal{O}(kb \cdot cost(\phi))$ and $\mathcal{O}(b^k \cdot cost(\phi))$, where b denotes beam size.

Figure 4 compares LVSA, CLMPT, and CQD-Beam on existential positive queries ($2p/3p/ip/pi/up$) in FB15k-237. Contrasted with CLMPT’s computationally intensive Transformer+GNN design, LVSA’s lightweight architecture achieves superior performance and efficiency, delivering 2–15x higher throughput than CQD-Beam with $b \geq 64$ while maintaining competitive MRR scores. Notably, CQD-Beam incurs out-of-memory (OOM) failures when $b \geq 512$ and $k \geq 2$ ($3p$ queries). Crucially, LVSA consistently outperforms baselines at equivalent computational costs, validating its capability to balance expressivity and scalability.

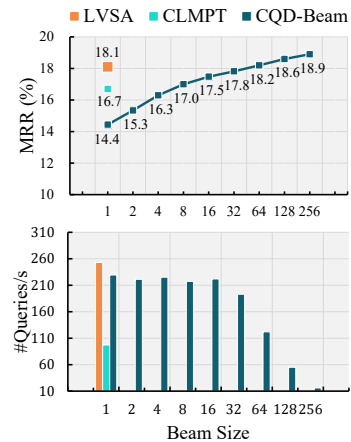


Figure 4: The performance and inference speed of LVSA, CLMPT, and CQD-Beam on FB15k-237.

Table 3: The MRR (%) results of our LVSA and ablation models on FB15k-237.

Model	A_n	$2in$	$3in$	inp	pin	pni
LVSA	10.9	12.4	18.3	8.5	7.3	8.0
w/o \mathcal{L}_{NS}	10.4	12.2	16.5	8.1	6.9	8.4
w/o \mathcal{L}_{NL}	7.6	7.4	13.9	7.0	5.1	4.5

6.5 Ablation Analysis

In this section, we conduct ablation studies to analyze the contributions of key components in LVSA. Specifically, we examine the impact of logic-driven regularization on the neural negator. As shown in Table 3, the ablation models LVSA w/o \mathcal{L}_{NS} and LVSA w/o \mathcal{L}_{NL} result in performance degradation of 0.5% and 3.3%, respectively. These results reveal the critical role of enforcing logical properties in embedding transformations for improving CQA performance. Notably, while geometry-aware Skolemization-based methods like BetaE and ConE theoretically satisfy logical axioms through specialized geometric operations (e.g., ConE’s sector complement for negation), their practical performance on queries involving negation remains suboptimal. Conversely, GNN-based approaches such as LMPNN and CLMPT struggle to incorporate logical constraints due to their black-box nature. This analysis highlights LVSA’s unique advantage in harmonizing explicit logical constraints with neural reasoning through differentiable regularization.

6.6 Analysis of Skolemization

This section provides an in-depth analysis of the effectiveness and interpretability of LVSA’s differentiable Skolemization module. As illustrated in Figure 5, we ground the existential variable embeddings of LVSA and the strongest Skolemization-based baseline CLMPT into concrete entities via the similarity metric, i.e., $V \approx \arg \max_{v \in \mathcal{V}} \phi_E(\varphi(V), \varphi(v))$. In this example, LVSA accurately grounds the existential variable to Computer (a science-aligned economic sector), while CLMPT erroneously associates it with a music album.

Table 4: The MRR (%) and H@1 (%) results of grounding existential variables for $2p$ queries.

Model	FB15k		FB15k-237		NELL995	
	MRR	H@1	MRR	H@1	MRR	H@1
LVSA	57.8	50.7	47.6	40.1	68.3	63.1
CLMPT	53.3	45.6	40.8	31.7	63.8	56.6

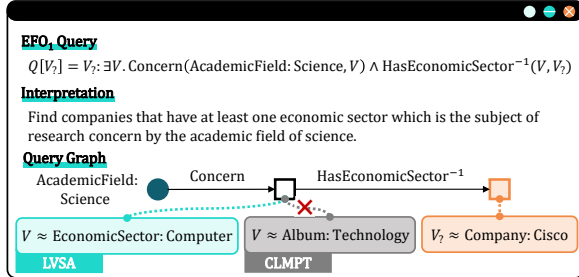


Figure 5: A sample of grounding the approximated Skolem function on NELL995.

Table 4 quantifies the grounding accuracy of LVSA and CLMPT across three benchmark datasets. Notably, LVSA achieves superior performance compared to CLMPT, particularly excelling in H@1 scores. These results empirically validate that LVSA’s differentiable Skolemization module operates not as a black-box neural network but as a logic-driven module that aligns symbolic reasoning with geometric constraints. Furthermore, the findings corroborate the analysis in the main results. Although CLMPT achieves a marginal performance advantage on $2p$ queries in FB15k, its reasoning process lacks the logical coherence exhibited by LVSA. Further analysis of interpretability can be found in Appendix H.

7 Conclusion

This work introduces the Grounding-Skolemization dichotomy, a formal framework exposing inherent limitations of prior CQA methods in balancing logic rigor and efficiency. We propose a novel Skolemization-based method LVSA that implements relational projection, conjunction, and fast querying as symbolic operations defined on a complex vector space. Besides, LVSA introduces a differentiable Skolemization module and logic-regularized neural negator to harmonize expressiveness with logic soundness. Empirically, LVSA achieves an optimal balance of logic rigor, inference efficiency, and interpretability compared to prior CQA approaches. Theoretically, LVSA guarantees universal expressivity for EFO₁ queries. Future work will explore enhancing the robustness and mitigating the local optima risk of the differentiable Skolemization module.

References

- [1] Bilal Abu-Salih and Salihah Alotaibi. A systematic literature review of knowledge graph construction and application in education. *Heliyon*, 10(3), 2024.
- [2] Erik Arakelyan, Daniel Daza, Pasquale Minervini, and Michael Cochez. Complex query answering with neural link predictors. In *ICLR*, 2021.
- [3] Erik Arakelyan, Pasquale Minervini, Daniel Daza, Michael Cochez, and Isabelle Augenstein. Adapting neural link predictors for data-efficient complex query answering. In *NeurIPS*, 2023.
- [4] Jiaxin Bai, Zihao Wang, Hongming Zhang, and Yangqiu Song. Query2particles: Knowledge graph reasoning with particle embeddings. In *Findings of NAACL*, pages 2703–2714, 2022.
- [5] Yushi Bai, Xin Lv, Juanzi Li, and Lei Hou. Answering complex logical queries on knowledge graphs via query computation tree optimization. In *ICML*, pages 1472–1491, 2023.
- [6] Yoshua Bengio, Jérôme Louradour, Ronan Collobert, and Jason Weston. Curriculum learning. In *ICML*, pages 41–48, 2009.
- [7] Kurt D. Bollacker, Colin Evans, Praveen K. Paritosh, Tim Sturge, and Jamie Taylor. Freebase: a collaboratively created graph database for structuring human knowledge. In *SIGMOD*, pages 1247–1250, 2008.
- [8] Antoine Bordes, Nicolas Usunier, Alberto García-Durán, Jason Weston, and Oksana Yakhnenko. Translating embeddings for modeling multi-relational data. In *NIPS*, pages 2787–2795, 2013.
- [9] Jiahang Cao, Jinyuan Fang, Zaiqiao Meng, and Shangsong Liang. Knowledge graph embedding: A survey from the perspective of representation spaces. *ACM Comput. Surv.*, 56(6):1–42, 2024.
- [10] Ines Chami, Adva Wolf, Da-Cheng Juan, Frederic Sala, Sujith Ravi, and Christopher Ré. Low-dimensional hyperbolic knowledge graph embeddings. In *ACL*, pages 6901–6914, 2020.
- [11] Xuelu Chen, Ziniu Hu, and Yizhou Sun. Fuzzy logic based logical query answering on knowledge graphs. In *AAAI*, pages 3939–3948, 2022.
- [12] Yihong Chen, Pasquale Minervini, Sebastian Riedel, and Pontus Stenetorp. Relation prediction as an auxiliary training objective for improving multi-relational graph representations. In *AKBC*, 2021.
- [13] Roy T Cook. *Dictionary of philosophical logic*. Edinburgh University Press, 2009.
- [14] E Knuth Donald et al. The art of computer programming. *Sorting and Searching*, 3(426-458):4, 1999.
- [15] Yanjun Gao, Ruizhe Li, Emma Croxford, John Caskey, Brian W Patterson, Matthew Churpek, Timothy Miller, Dmitriy Dligach, and Majid Afshar. Leveraging medical knowledge graphs into large language models for diagnosis prediction: Design and application study. *JMIR AI*, 4:e58670, 2025.
- [16] Cosimo Gregucci, Bo Xiong, Daniel Hernández, Lorenzo Loconte, Pasquale Minervini, Steffen Staab, and Antonio Vergari. Is complex query answering really complex? In *Forty-second International Conference on Machine Learning*, 2025.
- [17] William L. Hamilton, Payal Bajaj, Marinka Zitnik, Dan Jurafsky, and Jure Leskovec. Embedding logical queries on knowledge graphs. In *NeurIPS*, pages 2030–2041, 2018.
- [18] Michael Hersche, Mustafa Zeqiri, Luca Benini, Abu Sebastian, and Abbas Rahimi. A neuro-vector-symbolic architecture for solving raven’s progressive matrices. *Nat. Mac. Intell.*, 5(4):363–375, 2023.
- [19] Marvin Hofer, Daniel Obraczka, Alieh Saeedi, Hanna Köpcke, and Erhard Rahm. Construction of knowledge graphs: Current state and challenges. *Information*, 15(8):509, 2024.
- [20] Arthur B. Kahn. Topological sorting of large networks. *Commun. ACM*, 5(11):558–562, 1962.

- [21] Yuyin Lu, Hegang Chen, Yanghui Rao, Jianxing Yu, Wen Hua, and Qing Li. An efficient fuzzy system for complex query answering on knowledge graphs. *TechRxiv preprint: 10.36227/techrxiv.172833387.77152699/v1*, 2024.
- [22] Francois Luus, Prithviraj Sen, Pavan Kapanipathi, Ryan Riegel, Ndivhuwo Makondo, Thabang Lebese, and Alexander Gray. Logic embeddings for complex query answering. *arXiv preprint:2103.00418*, 2021.
- [23] Chau D. M. Nguyen, Tim French, Michael Stewart, Melinda Hodkiewicz, and Wei Liu. Spherical embeddings for atomic relation projection reaching complex logical query answering. In *WWW*, pages 35–46, 2025.
- [24] Maximilian Nickel, Lorenzo Rosasco, and Tomaso A. Poggio. Holographic embeddings of knowledge graphs. In *AAAI*, pages 1955–1961, 2016.
- [25] Maximilian Nickel, Volker Tresp, and Hans-Peter Kriegel. A three-way model for collective learning on multi-relational data. In *ICML*, pages 809–816, 2011.
- [26] Vilém Novák, Irina Perfilieva, and Jiri Mockor. *Mathematical principles of fuzzy logic*. Springer Science & Business Media, 2012.
- [27] Tony A Plate. Holographic reduced representations. *IEEE Trans. Neural networks*, 6(3):623–641, 1995.
- [28] Tony A Plate. *Holographic Reduced Representation: Distributed representation for cognitive structures*. CSLI Publications Stanford, 2003.
- [29] Hongyu Ren, Hanjun Dai, Bo Dai, Xinyun Chen, Denny Zhou, Jure Leskovec, and Dale Schuurmans. SMORE: knowledge graph completion and multi-hop reasoning in massive knowledge graphs. In *KDD*, pages 1472–1482, 2022.
- [30] Hongyu Ren, Weihua Hu, and Jure Leskovec. Query2box: Reasoning over knowledge graphs in vector space using box embeddings. In *ICLR*, 2020.
- [31] Hongyu Ren and Jure Leskovec. Beta embeddings for multi-hop logical reasoning in knowledge graphs. In *NeurIPS*, 2020.
- [32] Stuart J Russell and Peter Norvig. *Artificial intelligence: A modern approach*. Pearson, 2016.
- [33] Kenny Schlegel, Peer Neubert, and Peter Protzel. A comparison of vector symbolic architectures. *Artif. Intell. Rev.*, 55(6):4523–4555, 2022.
- [34] Zhiqing Sun, Zhi-Hong Deng, Jian-Yun Nie, and Jian Tang. Rotate: Knowledge graph embedding by relational rotation in complex space. In *ICLR*, 2019.
- [35] Kristina Toutanova and Danqi Chen. Observed versus latent features for knowledge base and text inference. In *CVSC*, pages 57–66, 2015.
- [36] Théo Trouillon, Johannes Welbl, Sebastian Riedel, Éric Gaussier, and Guillaume Bouchard. Complex embeddings for simple link prediction. In *ICML*, pages 2071–2080, 2016.
- [37] Jean Van Heijenoort. *From Frege to Gödel: A source book in mathematical logic, 1879–1931*. Harvard University Press, 1967.
- [38] Luke Vilnis. Geometric representation learning. *Doctoral Dissertation, University of Massachusetts Amherst*, 2021.
- [39] Zihao Wang, Yangqiu Song, Ginny Y. Wong, and Simon See. Logical message passing networks with one-hop inference on atomic formulas. In *ICLR*, 2023.
- [40] Wenhan Xiong, Thien Hoang, and William Yang Wang. Deeppath: A reinforcement learning method for knowledge graph reasoning. In *EMNLP*, pages 564–573, 2017.
- [41] Keyulu Xu, Weihua Hu, Jure Leskovec, and Stefanie Jegelka. How powerful are graph neural networks? In *ICLR*, 2019.

- [42] Hang Yin, Zihao Wang, and Yangqiu Song. Rethinking complex queries on knowledge graphs with neural link predictors. In *ICLR*, 2024.
- [43] Hao Yuan, Haiyang Yu, Shurui Gui, and Shuiwang Ji. Explainability in graph neural networks: A taxonomic survey. *IEEE Trans. Pattern Anal. Mach. Intell.*, 45(5):5782–5799, 2022.
- [44] Chongzhi Zhang, Zhiping Peng, Junhao Zheng, and Qianli Ma. Conditional logical message passing transformer for complex query answering. In *KDD*, pages 4119–4130, 2024.
- [45] Jing Zhang, Bo Chen, Lingxi Zhang, Xirui Ke, and Haipeng Ding. Neural, symbolic and neural-symbolic reasoning on knowledge graphs. *AI Open*, 2:14–35, 2021.
- [46] Yuan Zhang, Xin Sui, Feng Pan, Kaixian Yu, Keqiao Li, Shubo Tian, Arslan Erdengasileng, Qing Han, Wanjing Wang, Jianan Wang, et al. A comprehensive large-scale biomedical knowledge graph for ai-powered data-driven biomedical research. *Nat. Mac. Intell.*, pages 1–13, 2025.
- [47] Zhanqiu Zhang, Jie Wang, Jiajun Chen, Shuiwang Ji, and Feng Wu. Cone: Cone embeddings for multi-hop reasoning over knowledge graphs. In *NeurIPS*, pages 19172–19183, 2021.
- [48] Zhaocheng Zhu, Mikhail Galkin, Zuobai Zhang, and Jian Tang. Neural-symbolic models for logical queries on knowledge graphs. In *ICML*, pages 27454–27478, 2022.
- [49] Zhaocheng Zhu, Zuobai Zhang, Louis-Pascal A. C. Xhonneux, and Jian Tang. Neural bellmanford networks: A general graph neural network framework for link prediction. In *NeurIPS*, pages 29476–29490, 2021.

A Further analysis of prior CQA methods and our LVSA

The core analysis in the main text leverages our Grounding-Skolemization dichotomy to expose the trade-off between logic rigor and computational efficiency across current CQA methods, positioning our LVSA as a more efficient and transparent resolution for CQA, as illustrated in Figure 6a.

Complementing this theoretical discourse, here we synthesize the technical designs of prior methods, including embedding representations and logical operator modeling, to evaluate the symbolic implementation and varying degrees of symbolic integration, as visualized in Figure 6b. In contrast to conventional survey [45] that categorized CQA methods based on geometric embeddings as purely neural approaches, our analysis reveals their underappreciated symbolic dimensions and hybrid integration levels. This conceptual ambiguity reflects the blurred boundary in the neuro-symbolic taxonomy and highlights the critical value of our proposed Grounding-Skolemization dichotomy for systematically analyzing both current and emerging CQA methods.

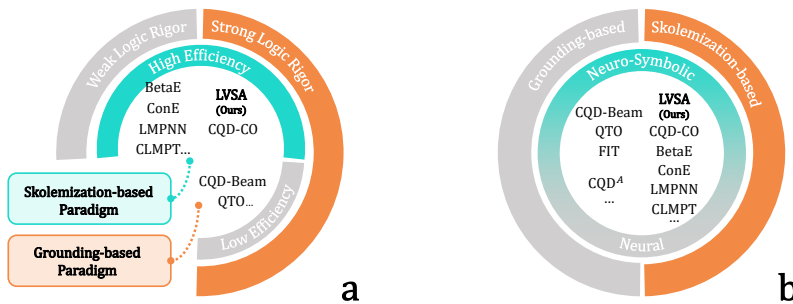


Figure 6: (a) Comparison of Skolemization-based and Grounding-based CQA methods in efficiency and logical rigor. (b) Taxonomy of CQA methods along the Grounding-Skolemization and Neuro-Symbolic dimensions.

A.1 Grounding-based Methods

The Grounding-based paradigm, pioneered by Arakelyan et al. [2], operates through atomic formula evaluation via neural link predictors [49, 36, 25] and truth value aggregation using fuzzy logic operators (e.g., Gödel t-norms [26]). Subsequent advancements include GNN-QE [48], which integrates

a GNN-based link predictor [49], and CQD^A [3] that enhances reasoning through neural adapter modules. Concurrently, SpherE [23] investigates the efficacy of diverse geometric embedding-based link predictors within the Grounding-based CQA framework. In parallel, Lu et al. [21] replace classical fuzzy operators with a fuzzy system, improving the capability of uncertainty handling through fuzzy rules. From the perspective of grounding algorithms, QTO [5] and FIT [42] guarantee global optimality through exhaustive candidate grounding, albeit at the cost of exponential time complexity. Instead, CQD-Beam [2] employs beam search to prune the candidate set, trading reasoning performance for tractability. Our evaluations on both standard [30] and new [16] benchmarks (Sections 6.2 and 6.3) show that Grounding-based methods excel at partially observable queries by leveraging an exhaustive search over known facts. However, they underperform on fully unobservable queries, indicating their lack of compositional reasoning capability.

A.2 Skolemization-based Methods

Although most CQA methods based on query embedding learning lack formal analysis of their logical foundations, their handling of existential variables can be conceptually aligned with neural approximations of Skolem functions. Current approaches are broadly categorized into geometric embedding methods and neural architecture-based methods.

Geometric embedding methods design geometrically structured embedding spaces (e.g., cones [47], boxes [30], and beta distributions [31]) based on set-theoretic principles [38], which encode logical inductive biases through geometric priors. Specifically, these methods represent existential variables as geometric embeddings of satisfiable solution sets and implement logical operators through algebraic transformations defined over the geometric space. For instance, ConE [47] employs cone-sector embeddings and models logical conjunction and negation via cone intersections and complements, respectively. FuzzQE [11] and LogicE [22] map (non-)variables to fuzzy set embeddings and model logical operations through fuzzy set operators in the embedding space. Despite their intuitive interpretability, these methods suffer from performance degradation due to misalignment between geometric priors and actual logical constraints, as well as optimization challenges arising from the complexity of geometric embeddings.

In contrast, neural architecture-based methods adopt simple vector embeddings and approximate Skolem functions through neural networks. CQD-CO [2] suffers from oversimplified Skolem approximations through random initialization of existential variable embeddings with naïve constraint optimization. Subsequently, LMPNN [39] and CLMPT [44] leverage Graph Isomorphism Networks (GINs) [41] to generate embeddings for existential variables via message passing over query graphs. While these GNN-based methods demonstrate enhanced performance by approximating Skolem functions via powerful GNNs, their black-box reasoning mechanisms fundamentally obscure logical transparency and prevent explicit constraint enforcement.

Table 5 compares the model architectures between representative Skolemization-based methods and our LVSA. Building upon VSA, our method employs complex-valued vectors to embed entities and relations. It utilizes simple yet powerful algebraic operations to model relation projection and logical conjunction, which offer both inference transparency and efficiency. Unlike GNN-based methods that simultaneously update all variable embeddings via message passing, LVSA’s sequential reasoning follows the topological ordering of the FOL query’s computation graph, thereby providing causal traceability and enhanced interpretability. To handle the more challenging components of the logical framework, including Skolem functions and logical negation, LVSA introduces logic-constrained neural modules.

B Connections between KGE models and VSA

Definition 3 (Knowledge Graph Embedding Models). *Given a KG, a Knowledge Graph Embedding (KGE) model maps entities and relations to an embedding space and defines a scoring function to measure triple plausibility.*

Definition 4 (Vector Symbolic Architecture). *A Vector Symbolic Architecture (VSA) is a computational framework that consists of a particular vector space and a set of algebraic operations defined on this space, including binding, unbinding, bundling, and a similarity measure.*

Table 5: Summary of representative Skolemization-based methods. **Bold** entries denote symbolic operations without neural components.

Model	Embedding Space Entity: $\varphi(e)$ Relation: $\varphi(r)$	Relation Projection	Existential Quantification	Conjunction	Disjunction	Negation	Similarity /Distance
Q2B [30]	vector: $\varphi(e) \in \mathbb{R}^d$ box: $\varphi(r) = (\text{Cen}(r), \text{Off}(r)) \in \mathbb{R}^{2d}$	addition	box	normalized addition + neural network	DNF	X	entity-to-box distance
BetaE [31]	beta distribution: $\varphi(e) = \text{Beta}(\alpha_e, \beta_e) \in \mathbb{R}^{2d}$	neural network	beta distribution	normalized addition + neural network	DNF	reciprocal	KL divergency
ConE [47]	cone: $\varphi(e) = (\theta_{\text{ax},e}, \theta_{\text{ap},e}) \in [0, 2\pi]^{2d}$ cone: $\varphi(r) = (\theta_{\text{ax},r}, \theta_{\text{ap},r}) \in [0, 2\pi]^{2d}$	addition + neural network	cone	normalized addition + neural network	DNF	complement	cone distance
FuzzQE [11]	fuzzy set: $\varphi(e) \in [0, 1]^d$	neural network	fuzzy set	t-norm	t-conorm	complement	cosine similarity
LogicE [22]	fuzzy set: $\varphi(e) = (l_e, u_e) \in [0, 1]^{2d}$ vector: $\varphi(r) \in \mathbb{R}^d$	neural network	fuzzy set	t-norm	t-conorm	complement	set distance
CQD-CO [2]	complex vector: $\varphi(e) \in \mathbb{C}^{2d}$ complex vector: $\varphi(r) \in \mathbb{C}^{2d}$	Hadamard product	complex vector	t-norm	t-conorm	complement	cosine similarity
LMPNN [39]	complex vector: $\varphi(e) \in \mathbb{C}^{2d}$ complex vector: $\varphi(r) \in \mathbb{C}^{2d}$	neural network	neural network	neural network	DNF	neural network	cosine similarity
CLMPT [44]	complex vector: $\varphi(e) \in \mathbb{C}^{2d}$ complex vector: $\varphi(r) \in \mathbb{C}^{2d}$	neural network	neural network	neural network	DNF	neural network	cosine similarity
LVSA (Ours)	complex vector: $\varphi(e) \in \mathbb{C}^{2d}$ complex vector: $\varphi(r) \in \mathbb{C}^{2d}$	Hadamard product	neural network	normalized addition	DNF	neural network	cosine similarity

Fundamentally, both KGE models [9] and VSAs [33] leverage embeddings of target objects for reasoning. KGE models focus on capturing semantics and structural patterns between entities and relations in KGs. Prior research has explored diverse embedding spaces (e.g., Hyperbolic space [10] and complex vector space [36, 34]) and scoring mechanisms (e.g., translation-based [8] and matching-based [36, 25] operations). While these models excel at link prediction, they typically lack support for first-order logical operations. In contrast, VSA has been predominantly applied to cognitive computing tasks [18], emphasizing the mapping of symbols into high-dimensional vectors while preserving compositional semantics through superposition operations. This enables efficient reasoning over compositions of basic symbols but lacks inherent mechanisms to model KG-specific relational patterns and formal logic.

Bridging the advantages of KGE models and VSAs, this work proposes LVSA for CQA, as detailed in Section 4. Specifically, LVSA aligns with ComplEx [36] in the designs of the embedding space and the triple scoring metric. In this way, LVSA establishes a novel paradigm that leverages pretrained KGE embeddings to enhance the performance of CQA, which is validated by both Grounding-based methods like CQD-Beam and Skolemization-based approaches like LMPNN. Beyond inheriting KGE models' capacity for relational semantic modeling, LVSA implements first-order logical operations through a neuro-symbolic integration of VSA-inspired algebraic operations with learnable neural modules. This hybrid architecture positions LVSA as both a generalization of KGE models for EFO₁ reasoning and an advancement of VSA for knowledge-aware symbolic computation.

C More details of implementation

Detailed Design of NormAdd: Given a conjunctive query $Q_\wedge = r_1(V'_1, V) \wedge \dots \wedge r_N(V'_N, V)$ as in Eq. (10), NormAdd operates as follows:

$$\bar{\varphi}(Q_\wedge) = \bar{\text{Re}}(Q_\wedge) + \bar{\text{Im}}(Q_\wedge)i = \frac{1}{N} \left[\sum_{j=1}^N \text{Re}(r_j \otimes V'_j) + \sum_{j=1}^N \text{Im}(r_j \otimes V'_j)i \right], \quad (21)$$

$$\varphi(Q_\wedge) = \text{Re}(Q_\wedge) + \text{Im}(Q_\wedge)i = \text{NormAdd}[\varphi(r_1 \otimes V'_1), \dots, \varphi(r_N \otimes V'_N)] = \frac{L}{\bar{L}} \cdot \bar{\varphi}(Q_\wedge),$$

where $\bar{L} = \frac{1}{2d} \sum_{m=1}^{2d} |\bar{v}_m|$ is the mean norm of the unnormalized mean vector $\bar{v} = [\text{Re}(\bar{\varphi}(Q_\wedge)); \text{Im}(\bar{\varphi}(Q_\wedge))]$, and $L = \frac{1}{2d \cdot N} \sum_{j=1}^N \sum_{m=1}^{2d} |v_{jm}|$ is the target norm, calculated as the mean norm of input vectors $v_j = [\text{Re}(\varphi(r_j \otimes V'_j)); \text{Im}(\varphi(r_j \otimes V'_j))]$.

Notably, for standard conjunction (without negation), we empirically observe $L \approx \bar{L}$, yielding $\varphi(Q_\wedge) \approx \bar{\varphi}(Q_\wedge)$. For cases involving negation such as Eq. (12), $\varphi(\neg(r_{N+1} \otimes V'_{N+1}))$ may

substantially reduce \bar{L} , in which normalization preserves consistent magnitude between inputs and the output by scaling with L/\bar{L} .

Detailed Design of Training Strategy: Based on the analysis in Appendix B, we initialize entity and relation embeddings in LVSA using pretrained ComplEx embeddings and then optimize the differentiable Skolemization module and neural negator. To mitigate the risk of local optima inherent to Skolemization’s satisfiability relaxation (Property 2a), we introduce a cross-entropy term over the in-batch candidate sets $\mathcal{V}_B = \{t \in A[Q]\}_{(Q,t) \in \mathcal{B}}$ to stabilize the training of the differentiable Skolemization module:

$$\mathcal{L}_{\text{CE}}(\mathcal{B}_{2p \wedge 3p}) = \frac{1}{|\mathcal{B}|} \sum_{Q \in \mathcal{B}} H(Q, \mathcal{V}) + H(Q, \mathcal{V}_B). \quad (22)$$

Following Chen et al. [12], we incorporate both entity prediction and relation prediction objectives in the primary loss function. Besides, we employ the Adam optimizer with an initial learning rate of $5e-4$ for each training stage.

D Case study of LVSA handling complex EFO₁ queries

Considering EFO₁ query $Q[V_?] = V_? : \exists V_1, V_2. r_1(V_1, V_2) \wedge r_2(h, V_2) \wedge r_3(V_2, V_?) \wedge r_4(V_2, V_?) \wedge r_5(h, V_?)$, the reasoning workflow of LVSA is structured as follows:

i. Topological Sorting of Query Graph:

As shown in Figure 7, the above EFO₁ query can be represented as a DAG (Query Graph). Using Kahn’s algorithm [20] for topological sorting, nodes are iteratively selected based on zero in-degree ($d = 0$), with edges removed post-selection. According to the selection order of nodes, we can derive a topological order $(V_1, h, V_2, V_?)$, which ensures dependency-preserving computation free of logical conflicts.

ii. Embedding Derivation:

Following the topological order, LVSA first generates embeddings for the independent existential variable V_1 and the anchor entity h , i.e., $\varphi(V_1) = \text{MLP}_1(\varphi(r_1))$ and $\varphi(h)$.

Then LVSA processes the dependent existential variable V_2 that exhibits both forward (F_D) and backward (B_D) logical dependencies:

$$F_D = \exists V_2 : r_1(V_1, V_2) \wedge r_2(h, V_2), \quad B_D = \exists V_2 : r_3(V_2, V_?) \wedge r_4(V_2, V_?). \quad (23)$$

Given $B_D \Rightarrow_* B_D^* = \exists V_2 : r_3^{-1}(V_{I,3}, V_2) \wedge r_4^{-1}(V_{I,4}, V_2)$, LVSA derives the embedding of V_2 by

$$\begin{aligned} \varphi(F_D) &= \varphi(r_1 \otimes V_1 + r_2 \otimes h), \\ \varphi(B_D) &= \varphi(r_3^{-1} \otimes V_{I,3} + r_4^{-1} \otimes V_{I,4}), \\ \varphi(V_2) &= \text{MLP}_D(\varphi(F_D) \oplus \varphi(B_D)). \end{aligned} \quad (24)$$

Finally, LVSA focuses exclusively on the subqueries involving the target variable $V_?$, that is, $r_3(V_2, V_?) \wedge r_4(V_2, V_?) \wedge r_5(h, V_?)$. The query embedding is derived through bundling operations:

$$\begin{aligned} \varphi(Q) &= \varphi(r_3 \otimes V_2 + r_4 \otimes V_2 + r_5 \otimes h) \\ &= \text{NormAdd}[\varphi(r_3 \otimes V_2), \varphi(r_4 \otimes V_2), \varphi(r_5 \otimes h)]. \end{aligned} \quad (25)$$

E More details of experimental settings

Details of Datasets: Table 6 summarizes key statistics of the three benchmark datasets, including the number of entities, relations, and training/validation/testing queries. Figure 8 illustrates the

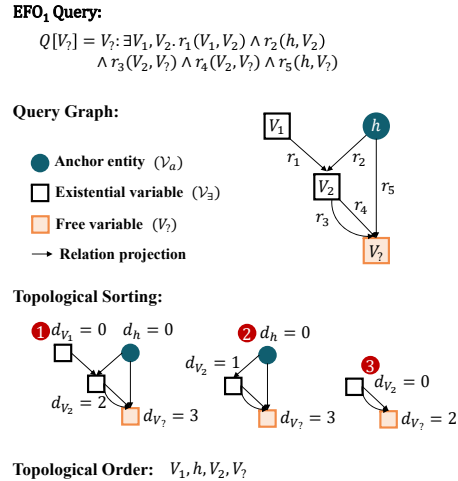


Figure 7: Diagram of the query graph and topological sorting workflow of the example query.

query graphs for all 14 complex query types. Notably, query types labeled with “ p ” (except the atomic query $1p$) contain existential quantifiers. Besides, the suffixes “ i ”, “ u ”, and “ n ” indicate the presence of logical conjunction, disjunction, and negation operations, respectively. Figure 9 presents a comparison of partially observable queries from the standard benchmarks and fully unobservable queries from the new benchmarks.

Table 6: Statistics of the three benchmark datasets.

Dataset	#Entity	#Relation	#Training Query		#Validation Query		#Testing Query	
			$1p/2p/3p/2in$	Others	$1p$	Others	$1p$	Others
FB15k	14,951	1,345	273,710	273,71	59,097	8,000	67,016	8,000
FB15k-237	14,505	237	149,689	149,68	20,101	5,000	22,812	5,000
NELL995	63,361	200	107,982	107,98	16,927	4,000	17,034	4,000

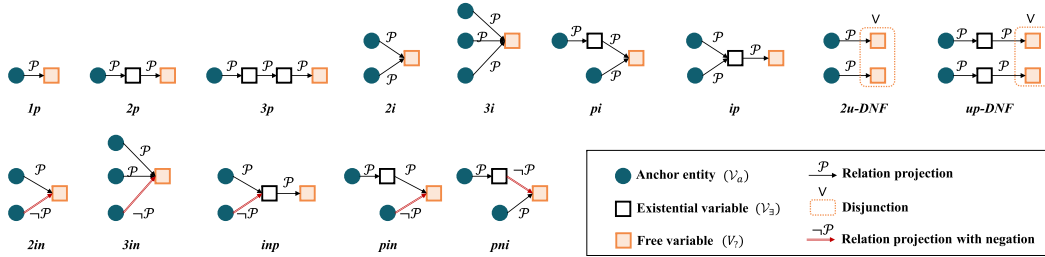


Figure 8: Query graph of each complex query type.

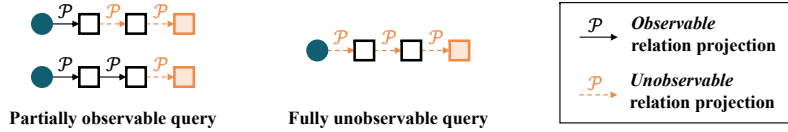


Figure 9: Samples of partially observable queries in the standard benchmarks and fully unobservable queries in the new benchmarks.

Details of Filtered MRR: Given a complex query $Q[V_?]$ with multiple answers $A[Q] \subseteq \mathcal{V}$, filtered MRR evaluates a model’s ability to rank every correct answer highly against non-answer entities. The filtered MRR is formally defined as follows:

$$\frac{1}{|A[Q]|} \sum_{a \in A[Q]} \frac{1}{\text{Rank}(a \mid \mathcal{V} \setminus A[Q])}, \quad (26)$$

where $\text{Rank}(a \mid \mathcal{V} \setminus A[Q])$ is the rank of answer a against all non-answer entities $\mathcal{V} \setminus A[Q]$.

F Sensitivity analysis of hyperparameters

Tables 7 and 8 evaluate hyperparameter robustness in LVSA’s differentiable Skolemization module and neural negator, respectively. These results indicate stable performance of LVSA across most configurations except sensitivity to the negation loss weight β (\mathcal{L}_{NL}).

G More details of significance test

We treat the MRR results of LVSA and Skolemization-based baselines on 14 types of complex queries across three benchmarks as data arrays, and perform one-tailed paired t-tests comparing LVSA against each baseline. The resulting p -values are summarized in Table 9. As demonstrated, LVSA achieves statistically significant superiority in reasoning performance over Skolemization-based baselines across all three benchmarks (p -values < 0.01).

Table 7: The MRR (%) scores of existential positive queries on FB15k-237, with differentiable Skolemization module under varying hyperparameter settings. Underline denotes the configuration used in main experiments.

MLP ₁			MLP _D		
$L = 1$	<u>$L = 2$</u>	$L = 3$	$L = 2$	<u>$L = 3$</u>	$L = 4$
18.0	18.1	18.0	17.6	18.1	18.1

Table 8: The MRR (%) scores of queries involving negation on FB15k-237, with neural negator under varying hyperparameter settings. Underline denotes the configuration used in main experiments.

MLP _N								
$\alpha = 0.1$	<u>$\alpha = 1$</u>	$\alpha = 10$	$\beta = 0.1$	<u>$\beta = 1$</u>	$\beta = 10$	$L = 1$	<u>$L = 2$</u>	$L = 3$
10.7	10.9	10.7	9.9	10.9	9.8	10.6	10.9	10.9

Table 9: The p -values of t-tests comparing LVSA against each Skolemization-based baseline.

Dataset	CQD-CO	BetaE	ConE	LMPNN	CLMPT
FB15k	6e-6	2e-7	2e-6	9e-4	7e-3
FB15k-237	7e-5	2e-6	3e-6	1e-5	2e-5
NELL995	4e-5	1e-7	2e-7	2e-4	9e-5

H Further analysis of interpretability

As an extension to Section 6.6, we propose to evaluate interpretability at two granularities: **(i) Variable-level:** measuring MRR for correctly grounding existential variables to valid intermediate entities, and **(ii) Path-level:** verifying complete reasoning paths when all variables are grounded to highest-confidence entities. Specifically, consider a $3p$ query $Q[V_?] = V_? : \exists V_1, V_2 : r_1(e_h, V_1) \wedge r_2(V_1, V_2) \wedge r_3(V_2, V_?)$, where e_h is the anchor entity. Firstly, we measure whether the model grounds each existential variable (i.e., V_1 and V_2) to a correct intermediate entity. For instance, if V_1 is grounded to e_1 , we check the validity of the sub-query $\exists V_2, V_? : r_1(e_h, e_1) \wedge r_2(e_1, V_2) \wedge r_3(V_2, V_?)$. Secondly, we measure the precision of the entire reasoning path when grounding all existential variables (V_1, V_2) and the target variable ($V_?$) to their highest-confidence entities (e.g., e_1, e_2, e_a), verifying if the full path $r_1(e_h, e_1) \wedge r_2(e_1, e_2) \wedge r_3(e_2, e_a)$ holds.

As shown in Table 10, LVSA performs comparably to CLMPT on grounding V_1 . However, LVSA significantly outperforms CLMPT on grounding V_2 and, critically, on the precision of the complete reasoning path. This demonstrates LVSA’s architectural stability in multi-step reasoning, while CLMPT exhibits substantial degradation at deeper steps. Additionally, LVSA’s transparent computation enables consistent end-to-end verification. The black-box nature of GNN-based methods obscures error attribution in CLMPT, further validating LVSA’s interpretability superiority for CQA.

Table 10: The MRR (%) results of quantitative interpretability evaluation on $3p$ queries.

Dataset	Model	Variable-level			Path-level
		V_1	V_2	Avg.	
FB15k	LVSA	60.2	40.1	50.2	40.7
	CLMPT	63.5	35.3	49.4	38.0
FB15k-237	LVSA	52.4	31.5	42.0	34.4
	CLMPT	49.3	23.8	36.6	19.0
NELL995	LVSA	61.7	47.1	54.4	57.6
	CLMPT	62.3	45.1	53.7	38.9